HHS Public Access

Author manuscript

J Comp Neurol. Author manuscript; available in PMC 2016 December 15.

Published in final edited form as:

J Comp Neurol. 2015 December 15; 523(18): 2752–2768. doi:10.1002/cne.23814.

Identification of B6SJL mSOD1^{G93A} mouse subgroups with different disease progression rates

Melissa M. Haulcomb[1,2,3,4,*], **Nichole A. Mesnard-Hoaglin**[1,2], **Richard J. Batka**[3,4], **Rena M. Meadows**[3,4,5], **Whitney M. Miller**[3,4], **Kathryn P. McMillan**[3,4], **Todd J. Brown**[3,4], **Virginia M. Sanders**[6], and **Kathryn J. Jones**[3,4]

[1]Neuroscience Program, Loyola University Medical Center, Maywood, Illinois, 60153

[2]Research and Development Service, Hines Veterans Administration Hospital, Hines, Illinois, 60141

[3]Anatomy & Cell Biology Department, Indiana University School of Medicine, Indianapolis, Indiana, 46202

[4]Research and Development Service, Roudebush Veterans Administration Medical Center, Indianapolis, Indiana, 46202

[5]Program in Medical Neurosciences, Indiana University School of Medicine, Indianapolis, Indiana, 46202

[6]Department of Molecular Virology, Immunology, & Medical Genetics, The Ohio State University, Columbus, Ohio, 43210

Abstract

Disease progression rates among patients with amyotrophic lateral sclerosis (ALS) vary greatly. While the majority of affected individuals survive three – five years following diagnosis, subgroups undergo a more rapidly progressing form, surviving less than one year, or slower progressing forms surviving for nearly 50 years. Genetic heterogeneity and environmental factors pose significant barriers in investigating patient progression rates. Similar to humans, variation in survival within the mSOD1 mouse has been well-documented, but different progression rates have not been investigated. In the present study, we identified two subgroups of B6SJL mSOD1^{G93A} mice with different disease progression rates; fast (FPG) and slow progression groups (SPG), as evidenced by differences in the rate of motor function decline. In addition, increased disease-associated gene expression within the FPG facial motor nucleus confirmed the presence of a more severe phenotype. We hypothesized that a more severe disease phenotype could be the result of 1) an earlier onset of axonal disconnection with a consistent degeneration rate; or 2) a more severe or accelerated degenerative process. We performed a facial nerve transection axotomy in both mSOD1 subgroups, prior to disease onset, as a method to standardize the axonal disconnection. Instead of leading to comparable gene expression in both subgroups, this standardization did not eliminate the severe phenotype in the FPG facial nucleus, suggesting the FPG phenotype is the

Corresponding author: Melissa Haulcomb, Ph.D., Psychiatry Dept., 320 W 15th St., Bldg. NB, Rm. 314, Indianapolis, IN 46202. mhaulcom@iupui.edu.

Conflict of Interest Statement The authors declare that they have no conflict of interest.

result of a more severe or accelerated degenerative process. We theorize that these mSOD1 subgroups may be representative of the rapid and slow disease phenotypes often experienced in ALS.

Graphical abstract

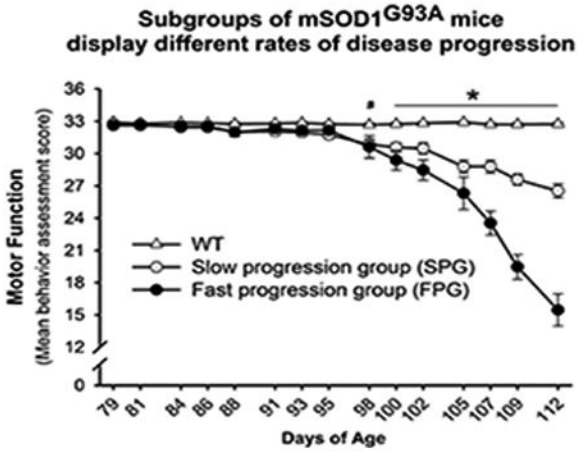

Indexing Terms

motoneuron; MN; facial nerve axotomy; mSOD1; ALS; disease progression; gene expression

Introduction

Amyotrophic lateral sclerosis (ALS) is the most common adult motoneuron (MN) degenerative disease that affects voluntary muscle movement and ultimately leads to respiratory failure and other pulmonary complications (Wijesekera and Leigh, 2009; Naganska and Matyja, 2011; Brooks et al., 2000). Initial symptoms often go unnoticed which delays diagnosis and makes identification of disease onset nearly impossible. Once symptoms have become apparent, the disease is often already entering final stages and severe MN degeneration has already occurred. Genetic studies have determined that a small portion of ALS cases are inherited, familial (fALS), while a majority (80-90%) are sporadic (sALS). Although mean survival is three – five years after diagnosis, subgroups of patients present with very rapid or slow disease progression rates, with life expectancies ranging from 1.5 years to more than 18 (Grohme et al., 2001, Ratovitski et al., 1999; Czaplinski et al., 2006).

While the etiology of ALS remains unknown, findings generated within the past few decades have advanced our understanding of the disease. The majority of these discoveries can be attributed to the first ALS mouse model developed in 1994, which overexpresses a common human mutant gene (mSOD1^{G93A}) encoding the enzyme, superoxide dismutase 1 (SOD1; Gurney et al., 1994; Saeed et al., 2009). mSOD1 mice display three distinct phases of disease, pre-symptomatic, symptomatic, and end-stage, which have been classically defined and consistently used throughout the literature. These phases are used as a point of reference for indicating the general phase of disease being studied, which is useful when

making comparisons across different mouse models that vary greatly in their age-related disease course (Gurney et al., 1994; Chiu et al., 1995). mSOD1^{G93A} mice appear to develop normally into adulthood and display a normal phenotype until approximately 90-100 days of age, when motor impairments become detectible, signifying symptom onset and defining the end of the pre-symptomatic stage. The progression of motor deficits throughout the symptomatic stage is accompanied by MN cell death that continues into end-stage where the MN loss reaches 50% in the ventral horn of the spinal cord (Chiu et al., 1995). Brainstem nuclei, such as the trigeminal, hypoglossal, and facial motor nuclei, are also affected but display significant MN loss during the late symptomatic stage or at end-stage (Nimchinsky et al., 2000; Chiu et al., 1995; Haenggeli and Kato, 2002; Niessen et al., 2006). While the pathology is well-documented, there is relatively high variability with regard to symptom onset and/or survival in the mSOD1^{G93A} mouse on the B6SJL hybrid background, compared to other background strains (Knippenberg et al., 2010; Haulcomb et al., 2014; Heiman-Patterson et al., 2011; Hamson et al., 2002; Heiman-Patterson et al., 2005). It has been suggested that this variability could be comparable to that which occurs among the ALS patient population, including fALS cases in which the same gene mutation is inherited (Abe et al., 1996; Maeda et al., 1997). Attempts have been made to identify potential causes of the various disease progression rates experienced by patients, such as environmental influences or potential genetic modifiers, however, this work is confounded by the heterogeneity inherent within the ALS population. Thus, we theorize that the B6SJL mSOD1^{G93A} mouse model is potentially useful for investigating disease progression rates.

According to the target disconnection (TD) theory of ALS, the initial pathology of the disease appears to be denervation of muscle endplates within the early pre-symptomatic stage (Fischer et al., 2004; Dadon-Nachum et al., 2011; Dupuis and Loeffler, 2009). Decreases in muscle mass and fiber diameter in mSOD1 mice follow and are likely a result of the loss of functional motor units (Marcuzzo et al., 2011). While compensatory axonal sprouting is evident, it appears to be inadequate as neuromuscular junction (NMJ) loss continues (Schaefer et al., 2005). By the time the mSOD1 mouse reaches the symptomatic stage, significant MN loss has already occurred (Chiu et al., 1995). Recent research in our laboratory supports the TD theory of ALS pathogenesis. Utilizing the facial motor nucleus, a homogenous population of MN (Ashwell, 1982), we observed a reliable and measureable molecular pattern which occurs throughout mSOD1 disease progression (Haulcomb et al., 2014). We successfully confirmed that this expression pattern in the mSOD1 facial nucleus is in response to disease-induced TD. By performing a facial nerve transection axotomy, prior to disease onset, we successfully replicated the disease-induced gene expression profile (Mesnard et al., 2011; Haulcomb et al., 2014). Thus, TD via axotomy provides a standardized experimental paradigm when superimposed on the mSOD1 mouse.

In the current study, we focused on investigating disease progression rates in the B6SJL mSOD1^{G93A} mouse. We hypothesize that distinct mSOD1 subgroups exist with different disease progression rates and, by using behavioral assessment and molecular analysis, we can identify these subgroups, thereby, providing a model to study the rapid and slow disease phenotypes often experienced by ALS patients.

The present study revealed two subpopulations of mSOD1 mice with differing disease progression rates; a fast progression group (FPG) and slow progression group (SPG). Enhanced progression of motor deficits and increased disease-induced molecular expression within the facial motor nucleus of the FPG, together, suggest a more severe disease phenotype in comparison to that of the SPG. In order to investigate the theory that a slower, less severe, disease progression rate coincides with prolonged target innervation or delayed TD onset, we performed a facial nerve axotomy to standardize the onset of axonal TD between the FPG and SPG. The facial nerve axotomy was performed on all mSOD1 mice within the pre-symptomatic stage prior to any disease-induced axonal TD. Subsequent analysis of the molecular profile within the axotomized facial motor nucleus, revealed that TD onset standardization did not lead to comparable gene expression changes between the two subgroups. These findings suggest that an earlier onset of the initial pathology, does not solely account for the differences in mSOD1 subgroups and that what distinguishes the groups is likely additional underlying disease mechanisms ultimately resulting in a more severe or accelerated degenerative process. Thus, the mSOD1 subgroups identified within this study present a unique opportunity to investigate the mechanisms responsible for the differences in disease susceptibility.

Materials and Methods

Animals

For all experiments, B6SJL WT (#100012; n = 31) and B6SJL transgenic mSOD1^{G93A} high copy number (B6SJL-Tg(SOD1-G93A)$_1$Gur; #002726; RRID:IMSR_JAX:002726; n = 32) mice were purchased from Jackson Labs (Bar Harbor, ME) at seven weeks of age. We used large groups of mice for the behavioral assessments as suggested by the recently updated guidelines for preclinical animal research in ALS (Ludolph et al., 2010; Ludolph et al., 2007).

All animal procedures were performed in accordance with institutional and National Institutes of Health guidelines on the care and use of laboratory animals for research purposes and approved by the Institutional Animal Care and Use Committee (IACUC). Mice were housed under a 12 hour light/dark cycle in autoclaved microisolator cages and provided autoclaved pellets and autoclaved drinking water ad libitum. The facility that housed the mice was equipped with a laminar flow system in order to maintain a pathogen-free environment. Mice were permitted to acclimate to their environment for one week before any procedures or testing was performed. Female mice were used for all experiments because of their reduced aggressive behavior, relative to males, during group housing.

Surgical Procedures

At 56 days of age, mice were fully anesthetized with 3% isoflurane inhalation and maintained at 2% isoflurane throughout the procedure. The right facial nerve was exposed at the level of the stylomastoid foramen and completely transected proximal to the bifurcation of the posterior and anterior auricular branches, as described previously (Serpe et al., 1999). Successful transections were verified by complete, unilateral loss of vibrissae movement and eye blink reflex on the ipsilateral side.

While both WT and mSOD1 mice received a right facial nerve axotomy and underwent behavioral analysis, only the mSOD1 mice, euthanized at 112 days of age, were assessed for facial motor nuclei mRNA expression as a secondary measure of disease severity among different mSOD1 subpopulations. The facial motor nuclei samples used for mRNA analysis of the mSOD1 subpopulations included the right, axotomized facial motor nucleus (surgically disconnected from muscular targets at 56 days of age) and the left, diseased facial motor nucleus (disconnected from muscular targets via disease-related mechanisms at an undetermined time point) were separately acquired from the same group of mice, as previously described (Haulcomb et al., 2014).

Behavioral Assessment

WT and mSOD1 mice (n = 31 and 32, respectively) were evaluated for motor deficiency three times per week, beginning at 79 days of age and ending at 112 days of age. A combination of six behavioral assessments were administered to analyze the onset and progression of motor impairments (Fig. 1). Tests were administered by the same animal handler and at the same time per testing day, approximately six hours into the light cycle. The order that the mice were tested was rotated every testing day and the mouse strain and identification information was coded by an uninvolved investigator prior to the onset of testing.

The **extension reflex test** assessed the mouse's ability to engage extensor or anti-gravity muscles in response to a tail suspension (elevation of 13cm, for five seconds; Feng et al., 2008; Irwin, 1968; Fig. 1A,G). We developed a scoring system that corresonded to the degree of limb extension. The scores were as follows: 7 = complete fore- and hind-limb extension; 6 = complete fore-limb extension, but only partial hind-limb extension; 5 = partial fore- and hind-limb extension; 2 = partial fore-limb extension, with no hind-limb extension, i.e. hind-limbs remained retracted; 0 = no fore- or hind-limb extension, thus, all limbs remained completely retracted.

The **paw-grip endurance test** was used as a measure of appendicular muscluar endurance (Combs and D'Alecy, 1987; Feng et al., 2008; Fig. 1B,H). Directly following the extension reflex test, mice were lowered onto the top of a plastic rodent cage lid (20cm × 46cm). After instinctively gripping the plastic grid with all four paws, the lid was rotated by the animal handler from the horizontal position to a vertical position for five seconds, then returned to the horizontal position. Capabilities for this task and the corresponding test scores were developed and are as follows: 5 = successfully grasps with fore- and hind-paws for five seconds; 4 = graps with fore- and hind-paws temporarily (less than five seconds), but grip release is suspected as an intentional drop as evidenced by all four paws releasing simultaneously and no attempt to grasp as the mouse falls; 3 = grasps with fore- and hind-paws temporarily, but release appears to be unintentional as mouse hangs by one or more paws or an obvious attempt is made to catch themselves as they slide down past the cage lid grid; 1 = grasps with fore-paws only for less than five seconds; 0 = unable to maintain grip with paws; thus, once lid is rotated vertically, the mouse falls instantaneously.

The **balance beam test** was administered to evaluate overall muscle strength and coordination as well as general vestibular and proprioceptive functioning (Feeney et al.,

1982; Combs and D'Alecy, 1987; Feng et al., 2008; Fig. 1C,I). We modified this test such that it assessed not only the ability of the mouse to remain on the beam, but also the ability to lift itself onto the beam. The wooden beam was constructed out of a thin piece of wood, 2.5cm wide and 76cm long, positioned at an elevation of 13cm. Versi-dry paper (Thermo Scientific Nalgene, #62065-00) covered the beam and was replaced as necessary to protect the wood. Each mouse was suspended by the tail and consistently positioned by the animal handler near and at a level slightly below the beam. At this position, the mouse is able to reach and grasp the beam with the fore-paws, at which point, the handler then releases the tail, by quickly lowering the mouse. The mouse is no longer suspended by the tail, but hanging on the beam and supporting its own body weight and from this point the mouse must pull its body onto the beam. Intentional drops or refusal to climb onto the beam after suspension release were not observed. Once on the beam, mice were observed for five seconds, traveling along the beam was not required. Scores used to gauge performance on this task were as follows: 5 = able to lift body onto beam with both fore- and hind-paws and did not fall off the beam throughout the test duration; 4 = only able to lift body onto the beam using the fore-paws and remains on the beam for test duration; 3 = only able to lift body onto beam using fore-paws and falls off the beam within five seconds; 1 = unable to lift body onto the beam, but once physically placed onto the beam, is able to remain on the beam for test duration; 0 = unable to lift body onto the beam and once physically placed onto the beam falls off within five seconds.

The remaining three tests were performed while mice were in an open field. Mice were individually placed within a clean, transparent, acrylic box (dimensions: 46cm × 33cm × 19cm) for two minutes. Versi-dry paper was placed at the bottom of the open field and was replaced between mice. The **gait analysis test** was a combination of observations related to forward mobility, gait and posture, that have been well-defined and routinely used within the literature (Knippenberg et al., 2010; Tada et al., 2011; Marcuzzo et al., 2011; Irwin, 1968; Fig. 1D,J). We previously published a scoring system that utilized a 7-point scale (Haulcomb et al., 2014), to evaluate symptom onset in mSOD1 mice, which was also used in the present study.

The **tail elevation test** evaluated the position of the tail relative to the body during forward locomotion (Irwin, 1968; Fig. 1E,K). Typically, during forward movement, the tail is relatively straight and held horizontally at the same or slightly higher than that of the body (Fig. 1D,E). This action utilizes the muscles at the base of the tail, which are innervated by coccygeal MN (Shinohara, 1999). The scoring system was modified and the corresponding observations included: 5 = tail elevation level is higher than or at the level of the body during forward movement; 3 = tail appears to slumps during forward movement, thus the distal portion of the tail is often at an elevation level which is lower than that of the body or routinely touches the ground; 0 = tail is not elevated during forward movement, i.e. the entire tail, or distal portion, drags on the ground for the duration of the test.

The **rearing behavior test** evaluates the ability to completely extend the hind-limbs during weight bearing behaviors such as rearing or raising up onto the hind-limbs (Irwin, 1968; Fig. 1F,L). Fortunately, B6SJL mice frequently and consistently rear or raise into an upright position onto their hind-limbs at the corners or walls of the open field box. It was interesting

that even severe motor impairment affecting the hind-limbs did not deter the mSOD1 mice from consistently attempting rearing behavior. Scores for this behavioral test were developed by our laboratory and are as follows: 5 = rearing behavior with complete extension/stretching of the hind-limbs, observed at least twice throughout the duration of the test; 4 = rearing behavior was not performed at all or was only observed once, regardless of whether the behavior revealed a complete or partial extension/stretch of the hind-limbs; 0 = rearing behavior with partial/incomplete extension/stretching of the hind-limbs was observed at least twice throughout the duration of the test.

All behavioral tests were directly scored by the animal handler at the time of test performance and in addition, all tests were video recorded for later analysis. The recordings were subsequently scored by two additional investigators for verification purposes. Each scoring scale or system for the individual behavior tests were specifically developed and optimized to provide a corresponding numerical value that is appropriately weighted for the functional motor impairment being assessing. The sum of all six test scores generated a motor score for each mouse per testing day, thus, providing a single quantitative measure, representing a comprehensive analysis of functional motor deficits.

Euthanasia Procedures

At 112 days of age or 56 days post-axotomy (dpa), WT mice (n = 31) and all but five randomly selected mSOD1 mice (n = 27) were euthanized by CO_2 asphyxiation in an isolated chamber followed by cervical dislocation. The brains were removed and flash-frozen, as previously described (Mesnard et al., 2010). The remaining five mSOD1 mice were permitted to progress to end-stage disease, without further behavioral assessments, for the purpose of verifying that the mSOD1 mice used in the current study succumbed to disease at an age that temporally coincides with that documented within the literature. mSOD1 mice were monitored daily for moribund criteria, which consisted of an inability to right themselves within 30 seconds after being placed on their side (Yang et al., 2011). Once these criteria were met, mice were euthanized by CO_2 asphyxiation. Post-tissue processing was not performed on end-stage mice in the current study.

Determination of symptom onset

Mean motor scores ± SEM for WT and mSOD1 mice, per testing day, were used to determine symptom onset. Statistical analysis was accomplished by using a two-way repeated measures analysis of variance (RM-ANOVA), followed by the Student-Newman-Keuls post hoc multiple comparison test, with significance at $P \leq 0.05$ (SigmaPlot, version 12.3; RRID:SciRes_000184). Symptom onset was identified for the purposes of defining the beginning of the symptomatic stage of disease among the current mSOD1 group.

Identification of mSOD1 subpopulations

Two, distinct statistical methods were employed to determine the existence of mSOD1 subgroups based on symptom progression rates. First, motor scores per mSOD1 mouse were averaged throughout the symptomatic stage (from 98 to 112 days of age). Next, a median split was performed for all 32 averaged motor scores in order to separate the mice into two groups. mSOD1 mice with averaged scores above the median were defined as the slow

disease progression group (SPG; n = 16), while mSOD1 mice with averaged scores below were identified as the fast disease progression group (FPG; n = 16).

A second statistical method was used to validate the previous findings and further refine the individual mSOD1 group assignments. The rate of motor function decline was calculated for each mSOD1 mouse based on the slope of the line from a simple linear regression of its motor scores across time throughout the symptomatic stage (from 98 to 112 days of age). Next, a two-step cluster analysis was performed to identify the optimal number of clusters of mice, and to determine where the spits should occur (IBM SPSS, version 22; RRID:rid_000042). The cluster analysis confirmed that a model with two clusters, provided an optimal fit to the data, based on Schwarz's Bayesian Criterion (BIC), indicating that there are in fact two subgroups of mSOD1 mice with different disease progression rates; SPG (n = 19) and FPG (n = 13). With only minor differences in the individual mSOD1 group assignments, the cluster analysis confirmed the presence of two distinct mSOD1 subgroups. The subgroup classification for individual mSOD1 mice identified by cluster analysis was used throughout the current study.

Analyses were performed between groups (WT, SPG, FPG) utilizing mean motor scores ± SEM, per testing day, and included a two-way RM-ANOVA, followed by the Student-Newman-Keuls post hoc multiple comparison test, with significance at $P \leq 0.05$ (SigmaPlot, version 12.3). Linear regression analysis was also performed using mean motor scores ± SEM during the symptomatic stage for mSOD1 subgroups (SigmaPlot, version 12.3). In order to test whether the two disease progression slopes were significantly different from one another we performed a linear mixed model, to account for the repeated measures of each mouse, using a 95% confidence interval (IBM SPSS, version 22).

In addition to regression analyses, a normality test (Shapiro-Wilk) was also executed using the rate of motor function decline for each mSOD1 mouse throughout the symptomatic stage (SigmaPlot, version 12.3). Since normality tests have little power to reject the null hypothesis when sample sizes are small (Ghasemi and Zahediasl, 2012), we increased the confidence interval to 90% for this particular test ($P \leq 0.10$).

Gene copy number analysis

We analyzed *Msod1* copy numbers to assess whether slight differences in copy number might account for the differences in disease progression rate, as it is well documented that large differences in copy number (i.e. high copy number mSOD1 mice vs. low copy number mSOD1) affects disease phenotypes and lifespan in the mSOD1^{G93A} mouse (Dal Canto and Gurney, 1995). Mouse DNA was isolated from a 0.5cm section of the tail using the Purelink Genomic DNA Mini Kit (Invitrogen, #K1820-00) and total DNA quantification was determined using a NanoDrop 2000 spectrophotometer. Transgene copy numbers were evaluated using semi-quantitative real-time reverse transcription-polymerase chain reaction (qPCR; Eppendorf Real-plex) by determining the ΔC_T of the transgene (*Msod1*) and a reference gene, *interleukin-2* (*Il2*), as previously described (Alexander et al., 2004; Heiman-Patterson et al., 2005). Previously published primer sequences (Alexander et al., 2004; Heiman-Patterson et al., 2005) were ordered from Bio-Synthesis, Inc. A linear regression

analysis was performed utilizing the *Msod1* $2^{-\Delta CT}$ vs. rate of motor score decline as a function of time throughout the symptomatic stage (SigmaPlot, version 12.3).

Laser microdissection

Twelve randomly selected mSOD1 brains (SPG, n = 7; FPG, n = 5) were cryosectioned at 25μm throughout the rostrocaudal extent of the facial motor nucleus, thaw-mounted onto glass polyethylene membrane-slides (Nuhsbaum #11505158), and stored at −80°C, as previously described (Haulcomb et al., 2014). Sides were individually fixed and stained for histological identification (Mesnard et al., 2011). The right (axotomized) and left (disease-only) facial motor nuclei were laser microdissected (Leica AS LMD) and separately collected into 65μl of extraction buffer (PicoPure RNA Isolation Kit, Invitrogen, #KIT0204), which had been added to the collection tube caps. Right and left facial motor nuclei samples were separately pooled for each mouse and stored at −80°C until RNA extraction was performed, as previously described (Haulcomb et al., 2014).

Analysis of mRNA expression

Total cellular RNA was isolated from laser microdissected samples using the PicoPure RNA Isolation Kit including a DNase treatment step (Qiagen, #79254), according to manufacturer's instructions. Total RNA quantification was determined using a NanoDrop spectrophotometer and concentrations were standardized prior to reverse-transcription. Complementary DNA was obtained using Superscript First Strand Synthesis System (Invitrogen, #11904-018), as previously described (Haulcomb et al., 2014).

PCR primer sets for the genes used in the current study were designed and custom ordered, as previously described (Haulcomb et al., 2014). qPCR was performed using the iCycler iQ detection system (Bio-Rad; Haulcomb et al., 2014). Relative mRNA expression levels were analyzed using the comparative C_T method and the endogenous housekeeping gene, *glyceraldehyde 3-phosphate dehydrogenase* (*Gapdh*; Sharma et al., 2010), resulting in the ΔC_T, which was then linearized, $2^{-\Delta CT}$ (Livak and Schmittgen, 2001, Schmittgen and Livak, 2008). Therefore, the relative quantity of mRNA expression per gene could be compared between mSOD1 groups (SPG vs. FPG). Comparisons were first performed between the left facial nuclei (disease-only) of mSOD1 subgroups (SPG vs. FPG). Second, and separately, comparisons were made between the axotomized or right facial nuclei of mSOD1 subgroups (SPG vs. FPG). All comparisons were restricted to individual genes and not made between genes, as previously described (Haulcomb et al., 2014). Statistical analysis was accomplished using a Student's t-test, two-tailed with significance reported as $P \leq 0.05$ (SigmaPlot, version 12.3).

Results

Behavioral assessment identifies the onset of the symptomatic stage in mSOD1 mice

The age of symptom onset was determined in order to define the end of the pre-symptomatic stage and beginning of the symptomatic stage among mSOD1 mice used in the current study. Behavioral tests (Fig. 1) were conducted three times per week yielding motor scores for WT and mSOD1 mice, beginning at 79 days of age and continuing until 112 days of age

(Supplemental Table 1). Statistical analysis revealed an overall main effect between WT and mSOD1 groups ($F_{1,960} = 421.61$; $P = \leq 0.05$), a main effect of age ($F_{14,960} = 40.45$; $P = \leq 0.05$), as well as an interaction between group × age ($F_{14,960} = 38.97$; $P \leq 0.05$). Motor scores were significantly different between WT and mSOD1 mice as early as 98 days of age ($P = \leq 0.05$; Fig. 2). Therefore, the battery of behavioral assessments used within the present study defined symptom onset at 98 days of age, which is consistent with previous findings (Haulcomb et al., 2014).

Behavioral assessment reveals two subgroups of mSOD1 mice, fast (FPG) and slow (SPG) progression groups

Motor scores for individual mSOD1 mice during the symptomatic stage (from 98 to 112 days of age) were used to identify two subpopulations of mSOD1 mice with different disease progression rates. Two, distinct statistical methods were employed to determine the existence of mSOD1 subgroups based on symptom progression.

Initially, motor scores for each individual mSOD1 mouse were averaged throughout the symptomatic stage. Next, a median split was performed in order to separate the mice into two groups, a slow disease progression group (SPG) and a fast disease progression group (FPG). Longitudinal analysis of mean motor scores between the SPG, FPG, and WT, revealed significant differences between groups (data not shown).

In order to confirm the existence of mSOD1 subgroups and refine the individual group assignments, initially predicted by the median split, we performed a two-step cluster analysis using the rate of motor function decline, for each mouse, throughout the symptomatic stage. The subsequent cluster analysis confirmed the presence of two mSOD1 subgroups with only minor differences in the individual mSOD1 group assignments; SPG (n = 19) and FPG (n = 13). Visualization of the distribution of mSOD1 motor decline rates suggests a bimodal distribution, with the presence of a heavy tail on the left side of the curve (Fig. 3). A normality test (Shapiro-Wilk) confirmed that the distribution was not normal ($P \leq 0.10$).Therefore, we conclude that the cluster analysis not only verifies the existence of the subgroups, originally identified using a median split, but also refined those subgroup assignments.

Longitudinal analysis of mean motor scores between the SPG, FPG, and WT, revealed significant differences between groups ($F_{2,945} = 422.08$; $P \leq 0.05$), age ($F_{14,945} = 119.43$; $P \leq 0.05$), and group × age ($F_{28,945} = 48.17$; $P \leq 0.05$). Pairwise comparisons between groups (SPG, FPG and WT), throughout the time course revealed statistical differences beginning at 100 days of age and continuing until the last testing day (Fig. 4A; Supplemental Table 1; $P \leq 0.05$). While comparisons between WT vs. SPG and WT vs. FPG at 98 days of age were significant ($P \leq 0.05$), mSOD1 subgroups (SPG vs. FPG) did not differ statistically at that time point. Linear regression analysis was also performed on the mSOD1 subgroups and resulted in a 3.375-fold increase in disease progression rate between the FPG (slope = -1.08; $R^2 = 0.580$) and the SPG (slope = -0.32; $R^2 = 0.294$; Fig. 4B). Therefore, using multiple statistical methods and a comprehensive battery of behavioral assessments, the current study has identified two mSOD1 subgroups with different symptom progression rates. While the SPG experienced a slow and steady decline in motor function during the symptomatic stage,

the FPG displayed a more severe phenotype as evidenced by the steep and rapid decline in motor function (Fig. 4B). Analysis via a linear mixed model reveals the slopes of the mSOD1 subgroups are statistically significant ($P < 0.001$). However, interestingly, both the SPG and FPG experienced symptom onset at the same time point (Fig. 4A; Supplemental Table 1).

Slight variations in transgene copy number do not correlate with motor scores

It is well-documented that large differences in *Msod1* transgene copy number, affect disease phenotypes and lifespan in the mSOD1 mouse models (i.e. high copy vs. low copy number mSOD1 mice; Dal Canto and Gurney, 1995). Therefore, we evaluated *Msod1* copy number in our mSOD1 mice to determine whether minor differences in transgene copy number could account for the variation in disease progression rates. Linear regression analysis revealed no correlation between *Msod1* copy number and rate of motor score decline throughout the symptomatic stage ($R^2 = 0.02$; $P = 0.59$; data not shown). Thus, our findings were consistent with others studying high copy number mSOD1 mice, that minor differences in copy number do not correlate to the differences in disease phenotypes and lifespan (Heiman-Patterson et al., 2005).

mSOD1 mice reach end-stage disease at an age consistent with that documented within the literature

The focus of the current study was to identify and characterize subpopulations of mSOD1 mice with different disease progression rates within the symptomatic stage. Since our euthanasia time point was within the symptomatic stage (112 days of age), we permitted a small number of mice to progress to end-stage to confirm that they succumbed to the disease as expected. All five mSOD1 mice that were permitted to progress to end-stage and were humanely euthanized at a mean age of 133 days with a standard deviation of ± 5 days (data not shown), which is consistent with that documented within the literature (Heiman-Patterson et al., 2005; Chiu et al., 1995).

Increased disease-induced molecular expression within the facial motor nucleus of the FPG suggests a more severe disease phenotype in comparison to that of the SPG

After identifying the mSOD1 subgroups based on symptom progression rates, we performed further analyses to confirm and characterize the two subpopulations of mSOD1 mice. As an additional, quantitative measure of disease progression, we analyzed and compared mRNA expression levels within the facial motor nuclei. We have previously shown that during disease progression the facial nucleus of mSOD1 mice reveals a reliable and measureable molecular response pattern across time (Haulcomb et al., 2014). This expression pattern, produced by a set of functionally diverse genes, is related to the disease process itself. Specifically, our previous work identified that the disease mechanism responsible for initiating this gene expression is axonal TD of the FMN (Haulcomb et al., 2014). Once disease-induced FMN TD has begun, relative mRNA expression levels within the mSOD1 facial nucleus increase and continue to rise over time. For a majority of the genes within the profile, higher mRNA expression levels are indicative of a more severe degenerative phenotype. Within the current study we analyzed the mRNA expression of 12 genes within

the facial motor nuclei of mSOD1 subgroups. While basic gene descriptions are included within the current results, more detailed descriptions, explanations and rationale for selection have been previously described (Mesnard et al., 2011; Haulcomb et al., 2014).

Glial-specific and glial-related gene expression

The first three genes analyzed are considered to be glial-specific or glial-related genes. Analysis of g*lial fibrillary acidic protein* (*Gfap*) and *cluster of differentiation 68* (*Cd68*) mRNA expression has been shown to be useful and reliable measures of the astrocytic and microglial responses, respectively (Jones et al., 1997; Streit et al., 1988; Graeber et al., 1990). In response to FMN TD, astrocytes and microglia become reactive, resulting in increases in *Gfap* and *Cd68* mRNA (Tetzlaff et al., 1988; Dissing-Olesen et al., 2007; Mesnard et al., 2011; Haulcomb et al., 2014). In addition, *fractalkine receptor* (*Cx3cr1*) mRNA expression is also elevated during mSOD1 disease-induced FMN TD (Haulcomb et al., 2014). CX3CR1 is expressed by microglia and plays an important neuroprotective role following to CNS injury (Chapman et al., 2000; Cardona et al., 2006). Gene expression analysis revealed a statically significantly increase in relative quantity mRNA levels in the facial nucleus of FPG mice compared to SPG mice for all three glial-related genes; *Gfap* (FPG: 1.086 ± 0.106 [data point range: 0.8312-1.4473]; SPG: 0.482 ± 0.0894 [data point range: 0.2558-0.9772]; $P = 0.001$; Fig. 5A), *Cd68* (FPG: 0.0196 ± 0.00291 [data point range: 0.0130-0.0295]; SPG: 0.0110 ± 0.00242 [data point range: 0.0020-0.0237]; $P = 0.045$; Fig. 5B), and *Cx3cr1* (FPG: 0.0251 ± 0.0036 [data point range: 0.0201-0.0285]; SPG: 0.0157 ± 0.0010 [data point range: 0.0108-0.0197]; $P < 0.001$; Fig. 5C).

TNFR1 death receptor pathway gene expression

We have previously shown that mSOD1 FMN TD results in a robust and sustained upregulation of genes involved in the tumor necrosis factor receptor 1 (TNFR1) pathway (Mesnard et al., 2011; Haulcomb et al., 2014). Assessment of *Tnfr1*, *Caspase-8*, and *Caspase-3* revealed increased relative quantity mRNA levels in the FPG facial nucleus in comparison to the SPG. Statistical analysis confirmed that increased mRNA expression in the FPG, compared to the SPG, was significant for the three genes involved in the TNFR1 death receptor pathway; *Tnfr1* (FPG: 0.0307 ± 0.00195 [data point range: 0.0254-0.0351]; SPG: 0.0238 ± 0.00093 [data point range: 0.0192-0.0260]; $P = 0.006$; Fig. 5D), *Caspase-8* (FPG: 0.0009 ± 0.0001 [data point range: 0.0007-0.0013]; SPG: 0.0006 ± 0.0001 [data point range: 0.0004-0.0009]; $P = 0.019$; Fig. 5E), and *Caspase-3* (FPG: 0.0022 ± 0.0001 [data point range: 0.0018-0.0025]; SPG: 0.0016 ± 0.0001 [data point range: 0.0011-0.0021]; $P = 0.021$; Fig. 5F).

Fas death receptor pathway gene expression

The role of the Fas death receptor (Fas) pathway in MN cell death during disease progression is well-documented in mSOD1 mice (Raoul et al., 2002, Raoul et al., 2006, Locatelli et al., 2007). Previously, we have analyzed mRNA levels of the Fas pathway in the mSOD1 facial motor nucleus throughout the pre-symptomatic and symptomatic stages of disease (Haulcomb et al., 2014). Interestingly, while the Fas pathway plays a major role in MN degeneration during the later stages of disease, the mRNA upregulation in response to

FMN TD is temporally delayed. Therefore, based on our previous understanding, regarding the time course of disease-induced FMN TD and the temporally delayed upregulation of Fas pathway genes following FMN TD, we expected mRNA expression levels to be near baseline at the time point analyzed within the current study (112 days of age). As anticipated, comparisons between the mSOD1 subgroups did not reveal differences in expression levels among genes involved in the Fas death receptor pathway; *Fas* (FPG: 0.0021 ± 0.0003 [data point range: 0.0013-0.0029]; SPG: 0.0016 ± 0.0003 [data point range: 0.0011-0.0030]; $P = 0.181$; Fig. 5G), *Fas-associated death domain* (*Fadd*; FPG: 0.0016 ± 0.0002 [data point range: 0.0011-0.0014]; SPG: 0.0015 ± 0.0001 [data point range: 0.0011-0.0020]; $P = 0.704$; Fig. 5H), or *neuronal nitric oxide synthase* (*Nnos*; FPG: 0.0004 ± 0.0001 [data point range: 0.0002-0.0005]; SPG: 0.0003 ± 0.00003 [data point range: 0.0002-0.0004]; $P = 0.279$; Fig. 5I).

Control gene expression

For control purposes, the molecular profile used within the current study also included a subset of genes that have been previously shown to remain unchanged in their expression levels during disease progression in the mSOD1 facial motor nucleus (Haulcomb et al., 2014). This subset of genes encodes the following intermediate signaling molecules; *death associated protein-6* (*Daxx*), *silencer of death domains* (*Sodd*), and *Tnfr1-associated death domain* (*Tradd*). As expected, mRNA expression of these genes was not different between the mSOD1 subgroups in the facial motor nucleus (data not shown) and were representative of baseline expression levels (Haulcomb et al., 2014).

In conclusion, utilizing mRNA expression analysis as a secondary measure of disease progression, the current results validate the behavioral findings. Together these data suggest that the FPG represents a subgroup of mSOD1 mice with a more severe disease phenotype in comparison to that of the SPG.

Standardizing the axonal target disconnection (TD) in the mSOD1 subgroups fails to abolish the increased gene expression in the FPG facial motor nucleus

As previously described, higher mRNA expression levels of glial-related and death receptor pathway genes in the mSOD1 facial nucleus, are indicative of a more severe degenerative phenotype (Hensley et al., 2002; Chen et al., 2004; Turner et al., 2004; Philips and Robberecht, 2011). It is likely that multiple disease-related mechanisms could explain the increased level of expression in the FPG facial nucleus. Increased expression may be a result of a more extensive axonal TD (i.e. more rapid or enhanced disease progression) or may indicate that a longer period of time has passed since the FMN were initially disconnect from their targets (i.e. earlier disease onset).

In order to investigate the possibility that the increased gene expression within the FPG facial nucleus is a result of an earlier disease-induced TD than that of the SPG, we standardized the FMN TD in the mSOD1 subgroups by performing a facial nerve transection axotomy prior to disease onset. The right facial nerve was completely transected at an early age (56 days of age), prior to any disease-induced FMN TD, therefore the time point of the surgical procedure marks the onset and completion of the TD process for the right facial

motor nucleus, as previously described (Mesnard et al., 2011; Haulcomb et al., 2014). Thus, this procedure standardizes the axonal TD onset and process for the MN in the right facial nerve and nucleus of both mSOD1 groups, while leaving all other aspects of disease progression unaffected; such as voluntary motor pathways of the spinal cord, left facial nucleus, etc.

At the time point of 56 days-post axotomy (dpa), or 112 days of age, mRNA expression of genes within the axotomized facial motor nuclei of mSOD1 subgroups were analyzed. It should be noted that while the mRNA expression within the axotomized facial nuclei is considered a response to the surgical procedure performed (FMN TD), the mSOD1 mouse does continue to undergo disease progression and therefore, we cannot rule out effects from additional disease mechanisms within the facial motor nucleus.

Glial-specific and glial-related gene expression

Analysis of glial-related gene expression revealed that mRNA levels for all genes were significantly higher within the axotomized facial nucleus of the FPG compared to that of the SPG; *Gfap* (FPG: 2.358 ± 0.407 [data point range: 1.2311-3.4027]; SPG: 1.241 ± 0.138 [data point range: 0.7071-1.9097]; $P = 0.014$; Fig. 6A), *Cd68* (FPG: 0.0350 ± 0.0050 [data point range: 0.0242-0.0532]; SPG: 0.0184 ± 0.0025 [data point range: 0.0113-0.0298]; $P = 0.008$; Fig. 6B), and *Cx3cr1* (FPG: 0.0411 ± 0.0036 [data point range: 0.0313-0.0496]; SPG: 0.0262 ± 0.0016 [data point range: 0.0221-0.0327]; $P = 0.002$; Fig. 6C). These results were surprising because the glial response to facial nerve axotomy is well-documented in both WT and mSOD1 mice (Jones et al., 1997; Streit et al., 1988; Graeber et al., 1990; Mesnard et al., 2011; Haulcomb et al., 2014) and the magnitude of the mRNA levels as well as the temporal expression pattern were thought to be closely regulated by the TD event itself. Since we had standardized the FMN TD onset between the two mSOD1 subgroups, we had expected the mRNA expression levels of glial-related genes to be similar.

TNFR1 death receptor pathway gene expression

Analysis of *Tnfr1*, *Caspase-8*, and *Caspase-3* revealed similar findings. Increased relative quantity mRNA levels were identified in the axotomized facial nuclei of the FPG vs. SPG for *Tnfr1* (FPG: 0.0385 ± 0.0018 [data point range: 0.0343-0.0442]; SPG: 0.0316 ± 0.0020 [data point range: 0.0211-0.0376]; $P = 0.034$; Fig. 6D) and *Caspase-8* (FPG: 0.0016 ± 0.0001 [data point range: 0.0013-0.0019]; SPG: 0.0011 ± 0.0002 [data point range: 0.0006-0.0017]; $P = 0.054$; Fig. 6E), as determined by a Student's t-test ($P \leq 0.05$). While there was a trend for increased expression of *Caspase-3* in the FPG, no statistical differences were evident (FPG: 0.0033 ± 0.0003 [data point range: 0.0025-0.0043]; SPG: 0.0026 ± 0.0003 [data point range: 0.0015-0.0038]; $P = 0.195$; Fig. 6F).

Fas death receptor pathway gene expression

As previously mentioned, Fas pathway gene expression is increased following FMN TD in mSOD1 mice, however, this upregulation is temporally delayed (Haulcomb et al., 2014). For this reason, the previously analyzed mSOD1 facial motor nuclei at 112 days of age (the left, disease-only facial nucleus), revealed baseline expression levels and thus, no measurable differences between the subgroups. However, the time course of FMN TD within the

axotomized or right facial nuclei differs from that of the left or disease-only facial nuclei previously analyzed. This difference is due to the surgically-induced FMN TD, which occurred much earlier than the FMN TD induced by the disease process alone (Marcuzzo et al., 2011; Haenggeli and Kato, 2002; Niessen et al., 2006; Chiu et al., 1995). Therefore, the period of time from FMN TD onset to mRNA analysis is significantly longer, with respect to the axotomized facial nuclei, and well within the timeframe necessary to identify and quantify increases in Fas pathway gene expression (Haulcomb et al., 2014).

As anticipated, mRNA levels of Fas pathway genes revealed upregulated expression in the axotomized facial nuclei of both mSOD1 subgroups compared to non-axotomized or disease-only facial nuclei, although these differences were not analyzed statistically. Comparisons between the axotomized facial nuclei of the mSOD1 subgroups confirmed the presence of increased expression of all three Fas pathway genes ($P \leq 0.05$) in the FPG vs. the SPG; *Fas* (FPG: 0.0039 ± 0.0006 [data point range: 0.0023-0.0053]; SPG: 0.0024 ± 0.0002 [data point range: 0.0021-0.0049]; $P = 0.021$; Fig. 6G), *Fadd* (FPG: 0.0032 ± 0.0003 [data point range: 0.0022-0.0039]; SPG: 0.0020 ± 0.0001 [data point range: 0.0017-0.0023]; $P = 0.002$; Fig. 6H), and *Nnos* (FPG: 0.0012 ± 0.0002 [data point range: 0.005-0.0017]; SPG: 0.0005 ± 0.0001 [data point range: 0.0003-0.0016]; $P = 0.016$; Fig. 6I).

Control gene expression

For control purposes, mRNA expression was analyzed for *Daxx*, *Sodd*, and *Tradd* within the axotomized facial nuclei of the mSOD1 subgroups. As expected, no differences in expression levels were detected (data not shown). Inclusion of these genes reveals that the increased mRNA expression consistently detected in the FPG facial motor nuclei, throughout this study, is not due to an overall non-specific increase in mRNA expression.

Discussion

It has been well documented that subgroups of ALS patients present with very rapid or slow disease progression rates (Grohme et al., 2001, Ratovitski et al., 1999). Investigating these differences in progression rates are confounded by genetic heterogeneity and environmental influences inherent within the patient population. Interestingly, several ALS mouse models also display relatively high variability, with regard to symptom onset and/or survival (Knippenberg et al., 2010; Haulcomb et al., 2014; Heiman-Patterson et al., 2011; Hamson et al., 2002). In particular, Hamson et al., 2002) noted that small groups of B6SJL SOD1^{G93A} mice revealed distinct differences in survival by meeting moribund criteria at two separate ages. A few years later, Heiman-Patterson T.D. et al. (2005) demonstrated that the variation in survival of the B6SJL SOD1^{G93A} mouse could be linked to the SJL background strain. Thus, it has been suggested that the SJL background may contain genetic modifiers or undetermined genes that interact with disease mechanisms resulting in either increased or decreased survival.

In the current study, we hypothesized that the variation in survival of the B6SJL mSOD1^{G93A} mouse could be a result of distinct mSOD1 subgroups with different disease progression rates or disease phenotypes. Identification of mSOD1 subgroups using

behavioral assessment would provide a model for investigating the rapid and slow progressing disease rates often experienced by ALS patients.

We developed a comprehensive battery of behavioral assessments, with a corresponding scoring system, to analyze various motor deficits in large group of mSOD1 mice, beginning in the pre-symptomatic stage (79 days of age). Comparisons made between WT and mSOD1 motor scores revealed symptom onset occurred at 98 days of age in mSOD1 mice, which is consistent with our previous findings (Haulcomb et al., 2014). Using individual mSOD1 motor scores generated throughout the symptomatic stage (98 to 112 days of age), we identified the presence of two subpopulations of mSOD1 mice with different rates of motor function decline; a fast (FPG) and a slow progression group (SPG). While the FPG experienced a steep and rapid decline in overall motor function throughout the symptomatic stage, the SPG displayed a less-severe, but consistent rate of decline. Two separate statistical methods were employed for the purposes of identifying potential subpopulations and both methods indicated the presence of two subgroups, with only minor differences in group assignments. Therefore, these results confirm the existence of two subpopulations of B6SJL mSOD1^{G93A} mice and show that with appropriate behavioral assessment methods these subgroups can be identified by their distinct disease progression rates.

We attribute the success of the behavioral assessment paradigm to three important factors. First, a sufficiently large mSOD1 group from which subpopulations could be identified (Ludolph et al., 2010; Ludolph et al., 2007). Second, frequent and consistent testing that generated sufficient and reliable data within a relatively short period of time, allowing us to identify and classify mSOD1 subgroups at a relatively early time point (112 days of age), with respect to the time course of disease. This opportunity for early, in vivo identification of subgroups is crucial for future studies aimed at investigating underlying mechanisms or potential treatments to slow disease progression.

Lastly, we attribute the success of the behavioral paradigm to the comprehensive nature of the various motor tasks included. We suspect that simple motor assessments alone would not be sufficient to accurately and reliably identify mSOD1 subgroups within the symptomatic stage of disease. The behavior paradigm developed within the current study involved a set of six assessments, which collectively tested a wide range of motor functions, each with a well-defined and weighted scoring system. We predict that the comprehensive nature of the behavioral assessments played an important role in the successful identification of the mSOD1 subgroups.

While the use of behavioral tests to determine disease progression rates in mSOD1 mice is relatively common and effective, physicians attempting to define progression rates in ALS patients have been less successful. For example, prognostic tests, such as isometric myometry of select muscle groups, administered at the time of diagnosis or shortly after have experienced limited success thus far and are unable to reliably predict disease progression rates or estimate life expectancy (Orrell et al., 1995; Armon and Brandstater, 1999). We theorize that a comprehensive battery of motor tests, consistently and frequently administered across time, similar in structure to the paradigm employed within the current study, would be more effective at predicting disease progression rates in ALS patients.

Subsequent to the identification of mSOD1 subgroups using rate of motor score decline, further analyses were performed to confirm and characterize the two subgroups. Gene expression levels within the facial motor nucleus were analyzed as an additional, quantitative measure of disease progression. Previous work performed by our laboratory has identified that a reliable and measureable molecular pattern occurs throughout disease progression the facial nucleus of mSOD1 mice (Haulcomb et al., 2014). In addition, we have verified that this expression pattern, produced by a set of functionally diverse genes, is in response to disease-induced axonal TD of the FMN (Haulcomb et al., 2014). Thus, once disease-induced FMN TD has begun (i.e. disease onset has occurred), mRNA expression levels increase and continue to rise over time. Genes analyzed within the current study were functionally grouped as follows: glial-related, death receptor pathway-associated, and control genes. In general, increased expression levels of glial-related and death receptor pathway-associated genes in the mSOD1 facial nucleus, are indicative of a more severe degenerative phenotype (Hensley et al., 2002; Chen et al., 2004; Turner et al., 2004; Philips and Robberecht, 2011).

We report that mRNA expression, for glial-related and TNFR1 pathway genes, was significantly increased in the FPG compared to that of the SPG. Providing additional confirmation of the severe disease phenotype displayed by the FPG. Although, while analysis of gene expression within the facial nucleus following disease-induced TD is a useful as a measure of disease progression, it does not provide any insights as to the underlying mechanism(s) or causes of the identified phenotype within the FPG. A variety of disease-related mechanisms may be responsible the increased expression levels in the FPG facial nucleus. Increased mRNA could be a result of a more extensive axonal TD (i.e. more rapid or enhanced disease progression) or may indicate that a longer period of time has passed since the FMN were initially disconnect from their targets (i.e. earlier disease onset). It is has been established, within the literature, that while the onset of FMN disease-induced TD is determined by disease-related mechanisms and occurs over a period of time, the time of TD onset is unknown and may not be consistent across animals (Schaefer et al., 2005; Niessen et al., 2006; Fischer et al., 2004). Based on the knowledge that disease-induced TD is often variable, and our understanding that the mRNA upregulation in response to FMN TD appears to be highly temporally-dependent, we considered that an earlier onset of disease-induced TD could readily account for the increased gene expression in the FPG. We tested this theory by controlling for potential differences in FMN TD onset between the two mSOD1 subgroups, which was accomplished by performing a right facial nerve transection axotomy to standardize the FMN TD within the pre-symptomatic stage, prior to any disease-induced FMN TD (i.e. prior to disease onset).

Our findings revealed consistent, increased mRNA expression of glial-related genes and death receptor pathway-associated genes within the axotomized facial nucleus of the FPG compared to that of the SPG. Therefore, standardization of the FMN TD onset failed to abolish the increased mRNA expression within the FPG, suggesting that the higher mRNA levels are a result of a more severe or accelerated degenerative process, and not solely due to an earlier disease-induced FMN TD onset, as was originally hypothesized. Interestingly, the behavioral data from the current study also supports this conclusion, as no differences in symptom onset were detected between the SPG and the FPG. Thus, we suspect that the onset

of disease mechanisms, such as disease-induced TD, may be consistent between the mSOD1 subgroups and that subsequent mechanisms involved in disease progression and MN degeneration may not be the same, and may explain the differences in phenotypes between the mSOD1 subgroups.

Future studies aimed at investigating additional disease mechanisms may help to explain the rapid progression of motor impairments in the FPG along with the increased levels of glial-specific and death receptor gene expression. Recent work in our laboratory has identified evidence that suggests the mSOD1 mouse may have a peripheral immune deficit (Mesnard et al., 2013; Mesnard-Hoaglin et al., 2014). It is well-established that the adaptive immune system plays an important role in mediating neuroprotection (Serpe et al., 1999; Xin et al., 2012). In addition, it is thought that this immune-mediated neuroprotection requires communication between T cells and resident CNS glial cells (Wainwright et al., 2009; Byram et al., 2004). Evidence of increased glial-reactivity or upregulated death receptor pathways may suggest a dysregulation in peripheral immune system and thus, a lack of neuroprotection. From this study we hypothesize that the heightened glial response along with increased expression of death receptor pathways represents a negative neuroinflammatory state within the microenvironment of the facial nucleus and may result in increased MN cell loss and/or a more severe disease phenotype in general.

In conclusion, we successfully identified two subgroups of B6SJL SOD1^{G93A} mice with different disease progression rates. Initial findings suggest that an earlier onset of disease is most likely not solely responsible for the different disease phenotypes presented by the mSOD1 subgroups. To our knowledge this is the first study to document and characterize the existence of mSOD1 subgroups with different disease phenotypes and provide a reliable methodology for identification. We predict that the mSOD1 subgroups will be a useful model to study the rapid and slow disease phenotypes often experienced by ALS patients.

Supplementary Material

Refer to Web version on PubMed Central for supplementary material.

Acknowledgments

Role of Authors: All authors had full access to all the data in the study and take responsibility for the integrity of the data and the accuracy of the data analysis. Study concept and design: MMH, NAM, VMS, KJJ. Acquisition of data: MMH, RJB, NAM. Analysis and interpretation of data: MMH, NAM, RMM, WMM, TJB, VMS, KJJ. Drafting of the manuscript: MMH. Critical revision of the manuscript for important intellectual content: MMH, VMS, KJJ. Statistical analysis: MMH, RJB. Obtained funding: VMS, KJJ. Administrative, technical, and material support: MMH, NAM, RJB, RMM, WMM, KPM, TJB. Study supervision: KJJ.

Grant sponsor: National Institutes of Health; Grant number: NS40433 (K.J.J. and V.M.S.).

Bibliography and References Cited

Abe K, Aoki M, Ikeda M, Watanabe M, Hirai S, Itoyama Y. Clinical characteristics of familial amyotrophic lateral sclerosis with Cu/Zn superoxide dismutase gene mutations. Journal of the neurological sciences. 1996; 136(1-2):108–116. [PubMed: 8815157]

Alexander GM, Erwin KL, Byers N, Deitch JS, Augelli BJ, Blankenhorn EP, Heiman-Patterson TD. Effect of transgene copy number on survival in the G93A SOD1 transgenic mouse model of ALS. Brain research Molecular brain research. 2004; 130(1-2):7–15. [PubMed: 15519671]

Armon C, Brandstater ME. Motor unit number estimate-based rates of progression of ALS predict patient survival. Muscle & nerve. 1999; 22(11):1571–1575. [PubMed: 10514236]

Ashwell KW. The adult mouse facial nerve nucleus: morphology and musculotopic organization. Journal of anatomy. 1982; 135(Pt 3):531–538. [PubMed: 7153172]

Brooks BR, Miller RG, Swash M, Munsat TL. El Escorial revisited: revised criteria for the diagnosis of amyotrophic lateral sclerosis. Amyotrophic lateral sclerosis and other motor neuron disorders: official publication of the World Federation of Neurology, Research Group on Motor Neuron Diseases. 2000; 1(5):293–299.

Byram SC, Carson MJ, DeBoy CA, Serpe CJ, Sanders VM, Jones KJ. CD4-positive T cell-mediated neuroprotection requires dual compartment antigen presentation. The Journal of neuroscience: the official journal of the Society for Neuroscience. 2004; 24(18):4333–4339. [PubMed: 15128847]

Cardona AE, Pioro EP, Sasse ME, Kostenko V, Cardona SM, Dijkstra IM, Huang D, Kidd G, Dombrowski S, Dutta R, Lee JC, Cook DN, Jung S, Lira SA, Littman DR, Ransohoff RM. Control of microglial neurotoxicity by the fractalkine receptor. Nature neuroscience. 2006; 9(7):917–924. [PubMed: 16732273]

Chapman GA, Moores K, Harrison D, Campbell CA, Stewart BR, Strijbos PJ. Fractalkine cleavage from neuronal membranes represents an acute event in the inflammatory response to excitotoxic brain damage. The Journal of neuroscience: the official journal of the Society for Neuroscience. 2000; 20(15):RC87. [PubMed: 10899174]

Chen LC, Smith A, Ben Y, Zukic B, Ignacio S, Moore D, Lee N. Temporal gene expression patterns in G93A/SOD1 mouse. Amyotrophic lateral sclerosis and other motor neuron disorders: official publication of the World Federation of Neurology, Research Group on Motor Neuron Diseases. 2004; 5(3):164–171.

Chiu AY, Zhai P, Dal Canto MC, Peters TM, Kwon YW, Prattis SM, Gurney ME. Age-dependent penetrance of disease in a transgenic mouse model of familial amyotrophic lateral sclerosis. Mol Cell Neurosci. 1995; 6(4):349–362. [PubMed: 8846004]

Combs DJ, D'Alecy LG. Motor performance in rats exposed to severe forebrain ischemia: effect of fasting and 1,3-butanediol. Stroke; a journal of cerebral circulation. 1987; 18(2):503–511.

Czaplinski A, Yen AA, Simpson EP, Appel SH. Slower disease progression and prolonged survival in contemporary patients with amyotrophic lateral sclerosis: is the natural history of amyotrophic lateral sclerosis changing? Archives of neurology. 2006; 63(8):1139–1143. [PubMed: 16908741]

Dadon-Nachum M, Melamed E, Offen D. The “dying-back” phenomenon of motor neurons in ALS. J Mol Neurosci. 2011; 43(3):470–477. [PubMed: 21057983]

Dal Canto MC, Gurney ME. Neuropathological changes in two lines of mice carrying a transgene for mutant human Cu,Zn SOD, and in mice overexpressing wild type human SOD: a model of familial amyotrophic lateral sclerosis (FALS). Brain research. 1995; 676(1):25–40. [PubMed: 7796176]

Dissing-Olesen L, Ladeby R, Nielsen HH, Toft-Hansen H, Dalmau I, Finsen B. Axonal lesion-induced microglial proliferation and microglial cluster formation in the mouse. Neuroscience. 2007; 149(1):112–122. [PubMed: 17870248]

Dupuis L, Loeffler JP. Neuromuscular junction destruction during amyotrophic lateral sclerosis: insights from transgenic models. Current opinion in pharmacology. 2009; 9(3):341–346. [PubMed: 19386549]

Feeney DM, Gonzalez A, Law WA. Amphetamine, haloperidol, and experience interact to affect rate of recovery after motor cortex injury. Science. 1982; 217(4562):855–857. [PubMed: 7100929]

Feng HL, Leng Y, Ma CH, Zhang J, Ren M, Chuang DM. Combined lithium and valproate treatment delays disease onset, reduces neurological deficits and prolongs survival in an amyotrophic lateral sclerosis mouse model. Neuroscience. 2008; 155(3):567–572. [PubMed: 18640245]

Fischer LR, Culver DG, Tennant P, Davis AA, Wang M, Castellano-Sanchez A, Khan J, Polak MA, Glass JD. Amyotrophic lateral sclerosis is a distal axonopathy: evidence in mice and man. Experimental neurology. 2004; 185(2):232–240. [PubMed: 14736504]

Ghasemi A, Zahediasl S. Normality tests for statistical analysis: a guide for non-statisticians. International journal of endocrinology and metabolism. 2012; 10(2):486–489. [PubMed: 23843808]

Graeber MB, Streit WJ, Kiefer R, Schoen SW, Kreutzberg GW. New expression of myelomonocytic antigens by microglia and perivascular cells following lethal motor neuron injury. Journal of neuroimmunology. 1990; 27(2-3):121–132. [PubMed: 2332482]

Grohme K, Maravic MV, Gasser T, Borasio GD. A case of amyotrophic lateral sclerosis with a very slow progression over 44 years. Neuromuscular disorders: NMD. 2001; 11(4):414–416. [PubMed: 11369195]

Gurney ME, Pu H, Chiu AY, Dal Canto MC, Polchow CY, Alexander DD, Caliendo J, Hentati A, Kwon YW, Deng HX, et al. Motor neuron degeneration in mice that express a human Cu, Zn superoxide dismutase mutation. Science. 1994; 264(5166):1772–1775. [PubMed: 8209258]

Haenggeli C, Kato AC. Differential vulnerability of cranial motoneurons in mouse models with motor neuron degeneration. Neuroscience letters. 2002; 335(1):39–43. [PubMed: 12457737]

Hamson DK, Hu JH, Krieger C, Watson NV. Lumbar motoneuron fate in a mouse model of amyotrophic lateral sclerosis. Neuroreport. 2002; 13(17):2291–2294. [PubMed: 12488813]

Haulcomb MM, Mesnard NA, Batka RJ, Alexander TD, Sanders VM, Jones KJ. Axotomy-induced target disconnection promotes an additional death mechanism involved in motoneuron degeneration in amyotrophic lateral sclerosis transgenic mice. The Journal of comparative neurology. 2014; 522(10):2349–2376. [PubMed: 24424947]

Heiman-Patterson TD, Deitch JS, Blankenhorn EP, Erwin KL, Perreault MJ, Alexander BK, Byers N, Toman I, Alexander GM. Background and gender effects on survival in the TgN(SOD1-G93A)1Gur mouse model of ALS. J Neurol Sci. 2005; 236(1-2):1–7. [PubMed: 16024047]

Heiman-Patterson TD, Sher RB, Blankenhorn EA, Alexander G, Deitch JS, Kunst CB, Maragakis N, Cox G. Effect of genetic background on phenotype variability in transgenic mouse models of amyotrophic lateral sclerosis: a window of opportunity in the search for genetic modifiers. Amyotrophic lateral sclerosis: official publication of the World Federation of Neurology Research Group on Motor Neuron Diseases. 2011; 12(2):79–86.

Hensley K, Floyd RA, Gordon B, Mou S, Pye QN, Stewart C, West M, Williamson K. Temporal patterns of cytokine and apoptosis-related gene expression in spinal cords of the G93A-SOD1 mouse model of amyotrophic lateral sclerosis. Journal of neurochemistry. 2002; 82(2):365–374. [PubMed: 12124437]

Irwin S. Comprehensive observational assessment: Ia. A systematic, quantitative procedure for assessing the behavioral and physiologic state of the mouse. Psychopharmacologia. 1968; 13(3): 222–257. [PubMed: 5679627]

Jones KJ, Kinderman NB, Oblinger MM. Alterations in glial fibrillary acidic protein (GFAP) mRNA levels in the hamster facial motor nucleus: effects of axotomy and testosterone. Neurochemical research. 1997; 22(11):1359–1366. [PubMed: 9355108]

Knippenberg S, Thau N, Dengler R, Petri S. Significance of behavioural tests in a transgenic mouse model of amyotrophic lateral sclerosis (ALS). Behav Brain Res. 2010; 213(1):82–87. [PubMed: 20450936]

Livak KJ, Schmittgen TD. Analysis of relative gene expression data using real-time quantitative PCR and the 2(-Delta Delta C(T)) Method. Methods. 2001; 25(4):402–408. [PubMed: 11846609]

Locatelli F, Corti S, Papadimitriou D, Fortunato F, Del Bo R, Donadoni C, Nizzardo M, Nardini M, Salani S, Ghezzi S, Strazzer S, Bresolin N, Comi GP. Fas small interfering RNA reduces motoneuron death in amyotrophic lateral sclerosis mice. Ann Neurol. 2007; 62(1):81–92. [PubMed: 17503505]

Ludolph AC, Bendotti C, Blaugrund E, Chio A, Greensmith L, Loeffler JP, Mead R, Niessen HG, Petri S, Pradat PF, Robberecht W, Ruegg M, Schwalenstocker B, Stiller D, van den Berg L, Vieira F, von Horsten S. Guidelines for preclinical animal research in ALS/MND: A consensus meeting. Amyotrophic lateral sclerosis: official publication of the World Federation of Neurology Research Group on Motor Neuron Diseases. 2010; 11(1-2):38–45.

Ludolph AC, Bendotti C, Blaugrund E, Hengerer B, Loffler JP, Martin J, Meininger V, Meyer T, Moussaoui S, Robberecht W, Scott S, Silani V, Van Den Berg LH. Preclinical EGftEoGftCo,

Proof of Concept Studies in ALSMNDM. Guidelines for the preclinical in vivo evaluation of pharmacological active drugs for ALS/MND: report on the 142nd ENMC international workshop. Amyotrophic lateral sclerosis: official publication of the World Federation of Neurology Research Group on Motor Neuron Diseases. 2007; 8(4):217–223.

Maeda T, Kurahashi K, Matsunaga M, Inoue K, Inoue M. [On intra-familial clinical diversities of a familial amyotrophic lateral sclerosis with a point mutation of Cu/Zn superoxide dismutase (Asn 86-Ser]. No to shinkei = Brain and nerve. 1997; 49(9):847–851. [PubMed: 9311004]

Marcuzzo S, Zucca I, Mastropietro A, de Rosbo NK, Cavalcante P, Tartari S, Bonanno S, Preite L, Mantegazza R, Bernasconi P. Hind limb muscle atrophy precedes cerebral neuronal degeneration in G93A-SOD1 mouse model of amyotrophic lateral sclerosis: A longitudinal MRI study. Experimental neurology. 2011; 231(1):30–37. [PubMed: 21620832]

Mesnard-Hoaglin NA, Xin J, Haulcomb MM, Batka RJ, Sanders VM, Jones KJ. SOD1(G93A) transgenic mouse CD4(+) T cells mediate neuroprotection after facial nerve axotomy when removed from a suppressive peripheral microenvironment. Brain, behavior, and immunity. 2014; 40:55–60.

Mesnard NA, Alexander TD, Sanders VM, Jones KJ. Use of laser microdissection in the investigation of facial motoneuron and neuropil molecular phenotypes after peripheral axotomy. Experimental neurology. 2010; 225(1):94–103. [PubMed: 20570589]

Mesnard NA, Haulcomb MM, Tanzer L, Sanders VM, Jones KJ. Delayed functional recovery in presymptomatic mSOD1 mice following facial nerve crush axotomy. Journal of neurodegeneration & regeneration. 2013; 4(1):21–25. [PubMed: 24672589]

Mesnard NA, Sanders VM, Jones KJ. Differential gene expression in the axotomized facial motor nucleus of pre-symptomatic SOD1 mice. The Journal of comparative neurology. 2011

Naganska E, Matyja E. Amyotrophic lateral sclerosis - looking for pathogenesis and effective therapy. Folia Neuropathol. 2011; 49(1):1–13. [PubMed: 21455838]

Niessen HG, Angenstein F, Sander K, Kunz WS, Teuchert M, Ludolph AC, Heinze HJ, Scheich H, Vielhaber S. In vivo quantification of spinal and bulbar motor neuron degeneration in the G93A-SOD1 transgenic mouse model of ALS by T2 relaxation time and apparent diffusion coefficient. Experimental neurology. 2006; 201(2):293–300. [PubMed: 16740261]

Nimchinsky EA, Young WG, Yeung G, Shah RA, Gordon JW, Bloom FE, Morrison JH, Hof PR. Differential vulnerability of oculomotor, facial, and hypoglossal nuclei in G86R superoxide dismutase transgenic mice. J Comp Neurol. 2000; 416(1):112–125. [PubMed: 10578106]

Orrell RW, King AW, Hilton DA, Campbell MJ, Lane RJ, de Belleroche JS. Familial amyotrophic lateral sclerosis with a point mutation of SOD-1: intrafamilial heterogeneity of disease duration associated with neurofibrillary tangles. Journal of neurology, neurosurgery, and psychiatry. 1995; 59(3):266–270.

Philips T, Robberecht W. Neuroinflammation in amyotrophic lateral sclerosis: role of glial activation in motor neuron disease. Lancet neurology. 2011; 10(3):253–263. [PubMed: 21349440]

Raoul C, Buhler E, Sadeghi C, Jacquier A, Aebischer P, Pettmann B, Henderson CE, Haase G. Chronic activation in presymptomatic amyotrophic lateral sclerosis (ALS) mice of a feedback loop involving Fas, Daxx, and FasL. Proceedings of the National Academy of Sciences of the United States of America. 2006; 103(15):6007–6012. [PubMed: 16581901]

Raoul C, Estevez AG, Nishimune H, Cleveland DW, deLapeyriere O, Henderson CE, Haase G, Pettmann B. Motoneuron death triggered by a specific pathway downstream of Fas. potentiation by ALS-linked SOD1 mutations. Neuron. 2002; 35(6):1067–1083. [PubMed: 12354397]

Ratovitski T, Corson LB, Strain J, Wong P, Cleveland DW, Culotta VC, Borchelt DR. Variation in the biochemical/biophysical properties of mutant superoxide dismutase 1 enzymes and the rate of disease progression in familial amyotrophic lateral sclerosis kindreds. Human molecular genetics. 1999; 8(8):1451–1460. [PubMed: 10400992]

Saeed M, Yang Y, Deng HX, Hung WY, Siddique N, Dellefave L, Gellera C, Andersen PM, Siddique T. Age and founder effect of SOD1 A4V mutation causing ALS. Neurology. 2009; 72(19):1634–1639. [PubMed: 19176896]

Schaefer AM, Sanes JR, Lichtman JW. A compensatory subpopulation of motor neurons in a mouse model of amyotrophic lateral sclerosis. The Journal of comparative neurology. 2005; 490(3):209–219. [PubMed: 16082680]

Schmittgen TD, Livak KJ. Analyzing real-time PCR data by the comparative C(T) method. Nature protocols. 2008; 3(6):1101–1108. [PubMed: 18546601]

Serpe CJ, Kohm AP, Huppenbauer CB, Sanders VM, Jones KJ. Exacerbation of facial motoneuron loss after facial nerve transection in severe combined immunodeficient (scid) mice. The Journal of neuroscience: the official journal of the Society for Neuroscience. 1999; 19(11):RC7. [PubMed: 10341268]

Sharma N, Marzo SJ, Jones KJ, Foecking EM. Electrical stimulation and testosterone differentially enhance expression of regeneration-associated genes. Experimental neurology. 2010; 223(1):183–191. [PubMed: 19427307]

Shinohara H. The musculature of the mouse tail is characterized by metameric arrangements of bicipital muscles. Okajimas folia anatomica Japonica. 1999; 76(4):157–169. [PubMed: 10565198]

Streit WJ, Graeber MB, Kreutzberg GW. Functional plasticity of microglia: a review. Glia. 1988; 1(5): 301–307. [PubMed: 2976393]

Tada S, Okuno T, Yasui T, Nakatsuji Y, Sugimoto T, Kikutani H, Sakoda S. Deleterious effects of lymphocytes at the early stage of neurodegeneration in an animal model of amyotrophic lateral sclerosis. Journal of neuroinflammation. 2011; 8(1):19. [PubMed: 21345177]

Tetzlaff W, Graeber MB, Bisby MA, Kreutzberg GW. Increased glial fibrillary acidic protein synthesis in astrocytes during retrograde reaction of the rat facial nucleus. Glia. 1988; 1(1):90–95. [PubMed: 2976741]

Turner MR, Cagnin A, Turkheimer FE, Miller CC, Shaw CE, Brooks DJ, Leigh PN, Banati RB. Evidence of widespread cerebral microglial activation in amyotrophic lateral sclerosis: an [11C] (R)-PK11195 positron emission tomography study. Neurobiology of disease. 2004; 15(3):601–609. [PubMed: 15056468]

Wainwright DA, Xin J, Mesnard NA, Politis CM, Sanders VM, Jones KJ. Effects of facial nerve axotomy on Th2- and Th1-associated chemokine expression in the facial motor nucleus of wild-type and presymptomatic mSOD1 mice. Journal of neuroimmunology. 2009; 216(1-2):66–75. [PubMed: 19818514]

Wijesekera LC, Leigh PN. Amyotrophic lateral sclerosis. Orphanet J Rare Dis. 2009; 4:3. [PubMed: 19192301]

Xin J, Mesnard NA, Beahrs T, Wainwright DA, Serpe CJ, Alexander TD, Sanders VM, Jones KJ. CD4+ T cell-mediated neuroprotection is independent of T cell-derived BDNF in a mouse facial nerve axotomy model. Brain, behavior, and immunity. 2012; 26(6):886–890.

Yang WW, Sidman RL, Taksir TV, Treleaven CM, Fidler JA, Cheng SH, Dodge JC, Shihabuddin LS. Relationship between neuropathology and disease progression in the SOD1(G93A) ALS mouse. Experimental neurology. 2011; 227(2):287–295. [PubMed: 21145892]

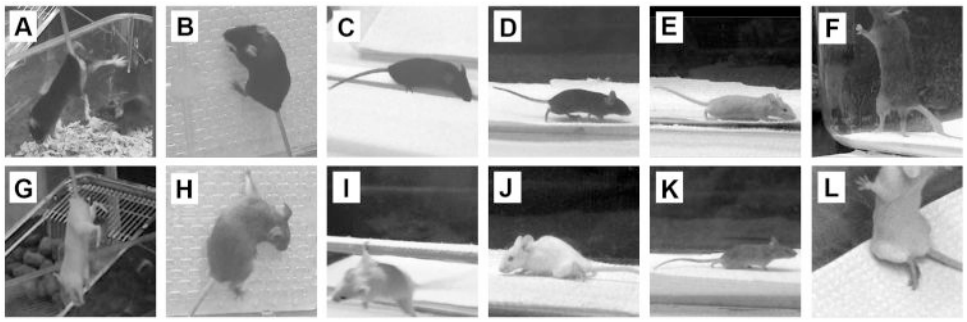

Figure 1.

A combination of six behavioral tests were used to evaluate the progression of motor deficits in WT (n = 31) and mSOD1^{G93A} (n = 32) mice. Images depict mice on various testing days (between 79 and 112 days of age) performing the following tasks: extension reflex (**A,G**), paw-grip endurance (**B,H**), balance beam (**C,I**), gait analysis (**D,J**), tail elevation (**E,K**), and rearing behavior (**F,L**). A defined scoring system (see Materials and Methods) was used to evaluate motor function. Top row images (A-F) are representative of normal motor function, or higher value scores, while bottom row images (G-L) represent severe motor deficits, or low value scores.

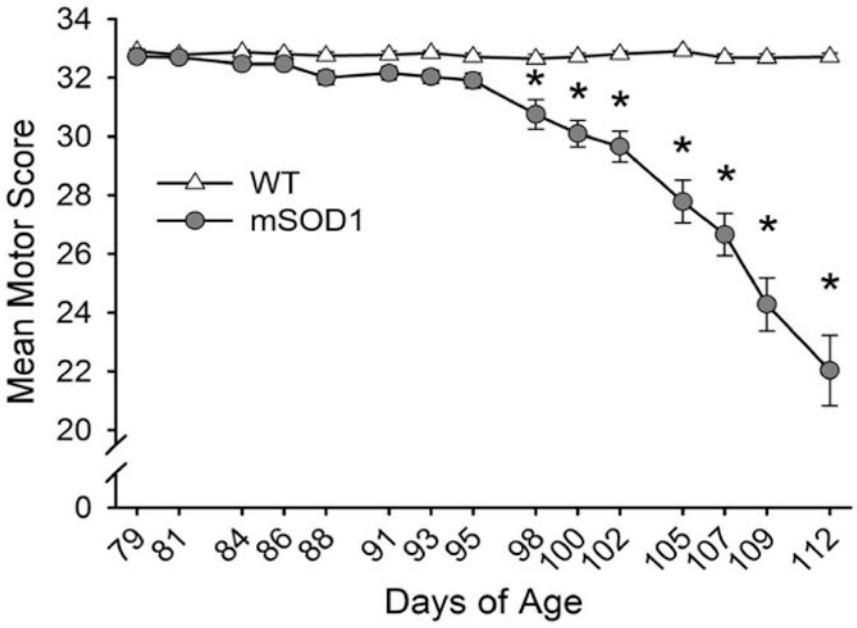

Figure 2.

Longitudinal analysis of motor deficits in mSOD1^{G93A} mice. WT (n = 31) and mSOD1 (n = 32) mice were evaluated for motor deficits across time. Behavioral assessment began at 79 days of age and continued 3 times per week until 112 days of age. Data are presented as mean motor score ± SEM. Symptom onset was identified at 98 days of age, marking both the end of the pre-symptomatic stage and the beginning of the symptomatic stage. Two-way repeated measures ANOVA (group × age) with Student-Newman-Keuls multiple comparison post hoc test: * represents a significant difference between WT and mSOD1, at $P \leq 0.05$.

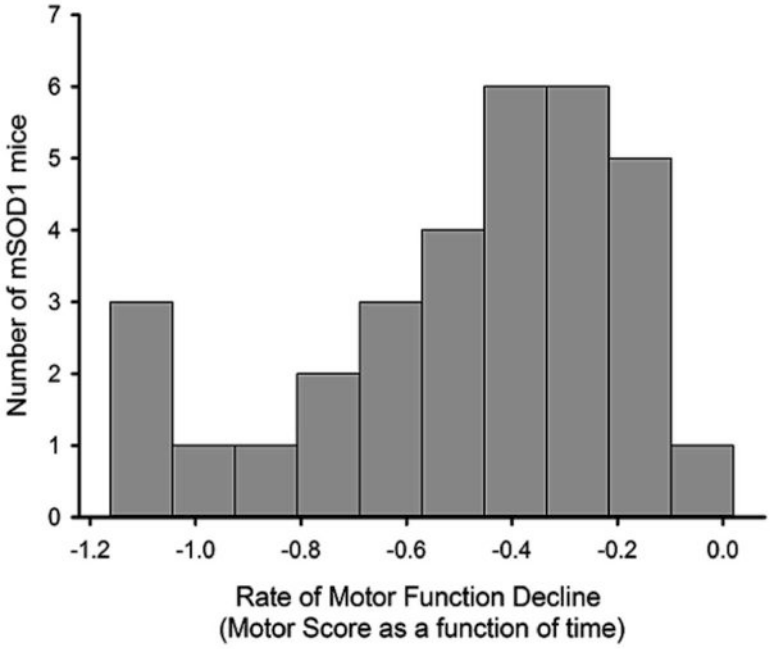

Figure 3.

Distribution of motor function decline. The rate or slope of motor function decline was calculated for individual mSOD1^{G93A} mice using motor scores across time during the symptomatic stage of disease (from 98 to 112 days of age).

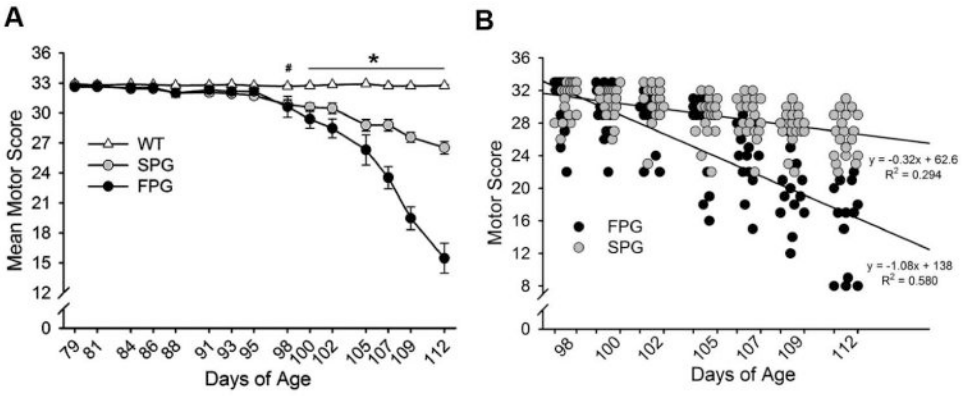

Figure 4.

Longitudinal analysis of two mSOD1^{G93A} groups with different disease progression rates, slow progression group (SPG) and fast progression group (FPG). **A:** Data are presented as mean score ± SEM across time. Two-way repeated measures ANOVA (group × age) with Student-Newman-Keuls multiple comparison post hoc test: * represents a significant difference between SPG (n = 19), FPG (n = 13) and WT (n = 31) mice; # represents a significant difference between WT and mSOD1 subgroups, at $P \leq 0.05$. **B:** Scatter plot of individual mSOD1 motor scores within the symptomatic stage of disease (from 98 to 112 days of age). X-axis variables were widened (days of age) to allow for visualization of overlapping data points. Linear regression analysis was performed separately on each mSOD1 subgroup, revealing a 3.375-fold difference in disease progression rates.

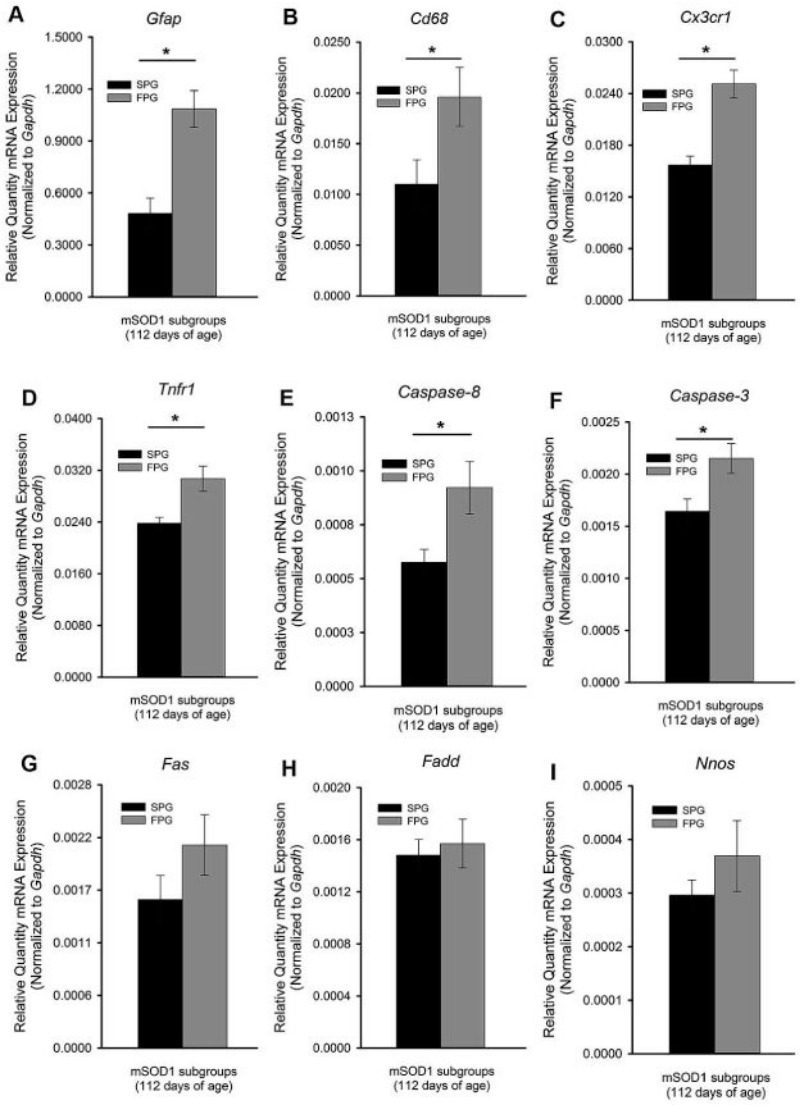

Figure 5.

Analysis of mRNA expression in the facial motor nucleus of mSOD1^{G93A} subgroups in response to disease-induced facial motoneuron (FMN) target disconnection (TD). The facial motor nuclei of mSOD1 subgroups, fast (FPG; n=5) and slow progression group (SPG; n=7), at 112 days of age, were analyzed for mRNA expression (mean ± SEM) for the following genes: *Gfap* (**A**), *Cd68* (**B**), *Cx3cr1* (**C**), *Tnfr1* (**D**), *Caspase-8* (**E**), *Caspase-3* (**F**), *Fas* (**G**), *Fadd* (**H**), and *Nnos* (**I**). Student's t-test: * represents a significant difference between subgroups, at $P \leq 0.05$.

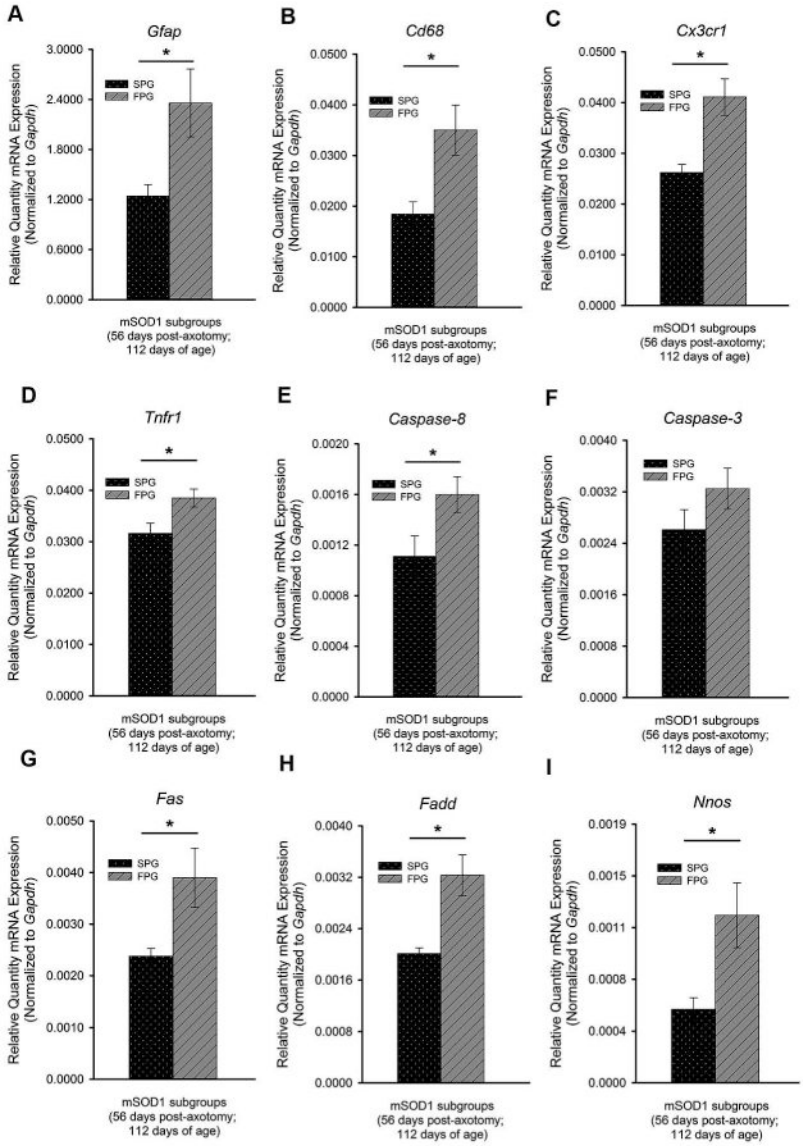

Figure 6.

Analysis of mRNA expression in the facial motor nucleus of mSOD1^{G93A} subgroups following standardization of axonal target disconnection (TD). Prior to disease onset a facial nerve transection axotomy was performed to standardize the onset of facial motoneuron (FMN) TD between the mSOD1 subgroups. The axotomized facial motor nuclei of mSOD1 subgroups, fast (FPG; n=5) and slow progression group (SPG; n=7), at 56 days post-axotomy (112 days of age), were analyzed for mRNA expression (mean ± SEM) for the following genes: *Gfap* (**A**), *Cd68* (**B**), *Cx3cr1* (**C**), *Tnfr1* (**D**), *Caspase-8* (**E**), *Caspase-3* (**F**), *Fas* (**G**), *Fadd* (**H**), and *Nnos* (**I**). Student's t-test: * represents a significant difference between subgroups, at $P \leq 0.05$.